



## Stanene/MnO<sub>2</sub> based micro-super capacitors a composite material for energy storage

A. Mary Juliet\*, Pranjal Dey and D. Jyothi Preshiya

Department of ETCE, Faculty of Electrical and Electronics, Sathyabama University, Chennai

### ABSTRACT

Micro-super capacitors are important on-chip micro-power sources for miniaturized electronic devices. Although the performance of micro-super capacitors has been significantly advanced by fabricating nanostructure materials, developing thin-film manufacture technologies and device architectures, their power densities remain far from those of electrolytic capacitors. Here we demonstrate the importance of synergistic effects between Stanene and molybdenum dioxide (MnO<sub>2</sub>) and their beneficial role as composites for Electrochemical Capacitors (ECs). Based on the first principle calculations, we find two-dimensional tin films, Stanene are Quantum Spin Hall (QSH) insulators that can be effectively tuned by chemical fictionalization and by external strain. First, introduction and the properties synthesis strategies and the use of Stanene is briefly given followed by a review on the preparation of Stanene/MnO<sub>2</sub> composite and finally the prospect and future challenges of it for energy storage are discussed.

**Keywords:** Quantum Spin hall, Micros Super Capacitor, Topological Insulator, Stanene

### INTRODUCTION

To satisfy the recent needs for renewable and sustainable power sources in modern electronic industry, recently many efforts are being made in developing energy storage devices which are light weight, flexible and environmental friendly in nature, such as capacitors and batteries. Super-capacitors, also called ultra-capacitors, bridge the differences between conventional and rechargeable batteries. They are the state-of-the-art energy storage devices which have become one of the most promising candidates for next-generation power devices because of their fast charging/discharging rate, high power density, sustainable cycling life (millions of cycles), and excellent cycle stability. Super capacitors provide up to 10,000 farads/1.2 volt, which is 10,000 times that of electrolytic capacitors, but it consumes half the power per unit time. To contrast, while super-capacitors have energy densities which is approximately 10% of the rechargeable batteries but their power density is generally 10 to 100 times greater. This leads to ultra-fast charge/discharge cycles than batteries. In recent years super-capacitors or electrochemical capacitors have attracted considerable interest as energy storage devices. Super capacitors or ultra-capacitors store charges only at the electrolyte-electrode interface of active materials through rapid reversible adsorption/desorption of ions.

The kind of the energy storage is defined by the following equation,

$$E = \frac{1}{2} cv^2 \quad (1)$$

Based on the charge-storage mechanism as mentioned in equation 1, super capacitors can be classified into two types- Electrical Double Layer Capacitor (EDLC) and Pseudo-capacitor. The EDLC is mainly dominated by electrostatic charge diffusion and accumulation at the interface of the electrode/electrolyte. This principle allows fast charging and discharging for a better performance. Pseudo-capacitors are governed by Faradic/Redox Reactions at the surface of electrode materials to accumulate specific capacitance. Both Double layer capacitance and pseudo capacitance contribute to the total capacitance value of a super capacitor. However, the ratio of the both can alter, depending on the design of the electrodes and the materials with which the electrolyte is composed of. Typically, super capacitors deliver a power density which is an order of magnitude larger ( $10,000 \text{ Wh Kg}^{-1}$ ) than that of lithium ion batteries, and an energy density that is two times of magnitude higher ( $10 \text{ Wh Kg}^{-1}$ ) than that of electrolytic capacitors.

As compared to the electrolytic capacitors they can have capacitance values of 10,000 times; up to 12,000 F at working voltages of 1.2 V. In terms of Specific power and energy, this gap covers several orders of magnitude. While existing super capacitors have energy densities that are approximately 10% of a conventional battery, their power density is about 10 to 100 times as great. This makes charging and discharging of super capacitors much faster than batteries. Additionally, they will bear many more charge and discharge cycles than batteries. Based on these storage mechanisms the electro-active materials used to fabricate super-capacitors are classified as Carbon based material, Conducting polymers, Metal-oxides/nitrides/hydroxides/sulphides. eg: Composite material like Graphene/ $\text{Mn}_3\text{O}_4$ ,  $\text{Co}_3\text{O}_4$ /Graphene, Sulphur/Graphene, Graphene/ $\text{MnO}_2$  & Sn/Graphene. Figure 1a states the electrochemical double-layer capacitance, where energy is stored by forming an EDL of electrolyte ions on the surface of conductive electrodes and Figure 1b pseudo-capacitance, where redox reactions occur close to the electrode surface.

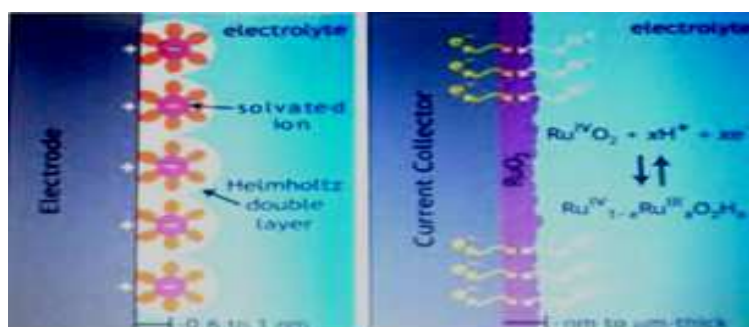


Fig 1a

Fig 1b

Figure 1 depicts the Schematic of charge storage in EDLCs

### I. Review of Micro Super-Capacitors

Currently, conventional lithography or inkjet /screen printing play an important role in fabrication of super capacitors [1]. However these techniques normally involve complicated lithographic process, toxic chemical treatments and harsh fabrication conditions thus resulting in high production cost. The limitation of these techniques motivates us to find out other simple, cheap and high output method to fabricate planar solid state super capacitors with high performance. Hence, we suggest a method to manufacture and design solid state micro-super capacitor. Micro-super capacitors represent one type of the newly developed miniaturized electrochemical energy storage devices.

Due to the *Short Ion Diffusion Length* they offer power densities that are many times larger in magnitude than those of conventional batteries and super capacitors. Various miniaturized electronic devices, such as micro batteries or energy –harvesting micro systems can be directly manufactured and integrated from these on chip micro devices, thereby providing excellent nano/micro-scale peak power [7,8]. In the recent past through the fabrication of nano structured electro active materials (such as carbide-derived carbon and carbon ions, amorphous nickel hydroxide), the development of thin-film manufacture technologies (such as electro chemical polymerization, in-situ reduction, co-precipitation, inject printing, and layer –by-layer assembly) and new device architectures, great efforts have been made to increase the energy and power densities of micro-super capacitors. To this end, it is essential to fabricate thin –film electrodes with a high electrical conductivity, advanced interfacial reliability of the main components

(electrode, separator electrolyte and substrate) with highly accessible electrochemically activated surface area, and an elaborate device structure with short ion diffusion pathways.

## II. Selection of Electrode Material for Micro super Capacitors

### 3. a) Existing material Manganese Dioxide

In recent years, Manganese oxide has drawn a considerable attention as its raw materials are abundant in nature; it is environmentally friendly, cost-effective, nontoxic with good electrochemical reactivity, environmental compatibility and high performance pseudo-capacitance. After its invention in 1865, the  $\text{MnO}_2$  as an electrode has been continuously improved. However, with the increasing demand to make higher capacity energy sources for the use in portable electronic devices has promoted an intensive research effort in developing new electrodes which are suitable for delivering high energy density. At a loading level of  $0.4\text{--}0.5\text{ mg cm}^{-2}$  the maximum specific capacitance (SC) for  $\text{MnO}_2$  is  $240\text{ F g}^{-1}$ . But, as per recent reports the theoretical specific capacitance of  $\text{MnO}_2$  is  $1370\text{ F/g}$  based on its charge storage mechanism. Redox reactions between the III and IV oxidation state of Mn ions involved in the pseudo capacitive (faradic) reactions occurring on the surface and in the bulk of the electrode is the major charge storage mechanism for manganese oxides. Hydrated manganese oxide exhibits a low specific capacitance of  $100\text{--}200\text{ Fg}^{-1}$  due to poor conductivity and lack of structural stability. However, due to its poor electric conductivity ( $10^{-5}\text{--}10^{-6}\text{ S/cm}$ ) such high theoretical capacitance has not been achieved in experiments. In addition, when the loading of  $\text{MnO}_2$  is in a high weight percentage in the electrode, the  $\text{MnO}_2$  is densely packed and then has only very limited accessible surface area for participating electrochemical charge storage process, which remarkably increases the contact resistance and in turn decreases the specific capacitance.

Therefore, to maximize utilization of the pseudo-capacity of  $\text{MnO}_2$ , keeping its thin film morphology while providing reliable electrical connection becomes one of the essential criteria in designing high-performance electrodes for  $\text{MnO}_2$ -based electrochemical super-capacitors. Such high values can only be obtained practically at very low loading levels for very thin layers of  $\text{MnO}_2$ . For such thin layers the utilization of material is high. So efforts are being made to enhance the utility by surfactant-mediated electro-deposition. An important way to increase the material utilization and thereby the specific capacitance is to decrease the particle size. Nanometer-sized particles of several materials have attracted considerable interest in recent years as the nano-particles are more favorable for technological applications than larger sized particles. The large surface-to-volume ratio in nano matters results in an increase in the chemical and electrochemical activity. In the regions of electrochemical reactions, which include solid-state diffusion process, nano particles are advantageous as they provide shorter diffusion path length as compared to the corresponding larger particles of the same matter.

In addition,  $\text{MnO}_2$  electrodes are found to be suffering from lack of structural stability and flexibility resulting in degraded long term electrochemical cycle life. An important consideration for overcoming the poor electronic conductivity, mechanical and chemical stabilities, and flexibility of  $\text{MnO}_2$  electrodes is to fabricate the electrode architecture via applying an ultra thin layer of  $\text{MnO}_2$  on the surface of a material that is having high surface area, is more porous and electronically conducting structure to shorten the solid state transport for ions and diffusion path lengths of electrons. Through this a good electrochemical performance can be obtained without sacrificing the mass-loading of the  $\text{MnO}_2$  phase.

### 3. b) Proposed Topological Insulator-Stanene

Tin and Tin based compounds have been extensively investigated as high capacity electrode materials for Li-ion batteries, Capacitor, and various other energy sources. Sn has mass of 2.67 times that of graphite is theoretically believed to provide  $994\text{mAhg}^{-1}$ . However, Sn atoms tend to aggregate during repeated cycling, which induces rapid loss of capacity of the electrode. Since graphene nano-sheets [2] are flexible and naturally conductive so it gives the idea of considering counterparts of graphene in group IVA (IV) and group VA (V) elements of the periodic table through which recent progress in search of new QSH insulators is being made. Among the group IV elements, although lead (Pb) possesses the largest spin-orbit coupling (SOC) strength but it is found out to be topologically trivial due to its freestanding one BL thick film. Turning to Sn, which is the group IV element with the second largest SOC strength. As compared to Si or Ge independent Sn exhibits a larger nontrivial band gap and has been the subject of a number of previous studies. Tin compounds  $\text{SnX}$  ( $\text{X} = \text{H, I, Br, Cl, F}$  or  $\text{OH}$ ) in one BL thick layers are predicted to be topological/QSH insulators, with the hydrogenated version called stanene.

The specialty of topological insulators is that by their very nature, they coerce electrons to move in defined lanes without any speed limit like an expressway as reported. As long as the electrons are on the free path of the edges or

surfaces, they will travel without resistance. Topological insulators are new states of quantum matter interesting for both fundamental condensed-matter physics and material science. Two-dimensional (2D) topological insulators [2] (TI) or quantum spin hall (QSH) insulators are characterized by the presence of gapless edge states protected by the constraints of time-reversal symmetry in an otherwise insulating bulk material, Whereas the surface states of three-dimensional topological insulators are not protected against scattering at any angle other than 180°. The spin-polarized conducting channels at the edges of a 2D-TI are free from backscattering, promising the robustness of conducting edge states as well as low power consuming applications. The chemical symbol of tin is Sn, originating from the Latin word “Stannum” for tin, therefore a monolayer of Sn film can be called “Stanene”, in analogy with graphene and silicon. The new material has been christened but not yet fabricated on a commercial scale. Stanene is a kind of ‘topological insulator’, which means its interior is an insulator but it conducts electrons along its surface. By making the monolayer of tin that is only a single atom thick, the Stanene is essentially all surface, which allows it to conduct electricity with 100 percent efficiency at temperatures up to 100 degrees Celsius.

These unusual properties result from complex interactions between the electrons and nuclei of heavy atoms in Stanene. Stanene has extraordinarily large bulk gaps (~0.3 eV), and by chemical functionalization and by external strain its QSH states can be effectively tuned, and their use is benefitted from the abundant degree of freedom in the chemical functional group. In contrast to the planar geometry of graphene, a low-buckled configuration of stanene is found to be more stable for stanene. For decorated stanene structures (like stanane), they have a stable sp<sup>3</sup> configuration similar to graphene, with the chemical functional groups alternating on both sides of the nano-sheet in their most stable configuration. The stability of the 2D tin films is further confirmed by phonon calculations which project that there is no imaginary frequency.

All this makes stanene intriguing for application. For example, by controlling the chemical functionalization, dissipation-less conduction “wires” could be patterned in an ultra-thin tin film of low power consumption electronics. To this day scientists are researching and trying to push the limits of various materials, channeling so much electricity through it that the material's electrical resistance causes the wires to heat up, potentially setting it on fire. If stanene fulfills its expectations & promises then chips could get smaller and faster without running this risk of overheating. Stanene could increase the speed and lower the power needs of future generations of computer chips. Compared to stanene, in decorated stanene the Sn-Sn bond length slightly increases, the buckling of the tin nano-sheet decreases which causes the enhancement of the equilibrium lattice constant. Compared to stanene, decorated (or functionalized) stanene structures offer much more possibilities which is clearly indicated in Figure 2.

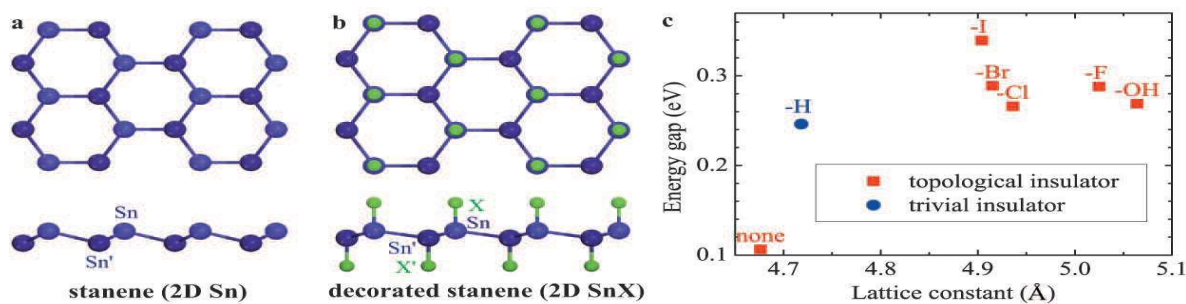


Figure 2 depicts the structure of Stanene

### III. Electrode Fabrication with the proposed Stanene Material

As described above, one of the intractable issues for the use of stanene as an electrode for various power sources is that the chemically derived stanene may suffer from agglomeration and re-stacking after the removal of dispersed solutions and drying due to the van der Waals interactions, thus consequently lowering the electrochemical performance of stanene for micro-supercapacitors [3]. To fully utilize the potential, cost-effectiveness, nontoxic with good electrochemical reactivity, environmental compatibility, high performance pseudo-capacitance and 100 percent efficiently conductive TI stanene, we propose the idea of fabricating Sn/MnO<sub>2</sub> electrode to overcome the mutual drawbacks and to form a next generation electrode material which we expect to be an effective and practical method. The aim is to maximize the practical use of the combined advantages of both stanene and MnO<sub>2</sub> as active materials for improving the electrochemical energy storage capacity and to lower or even solve the current electrode problems.

The active materials stanene and  $\text{MnO}_2$  [4] are pre-weighed before mixing them together. The weight ratio of stanene varies in relation to the conductivity of the active materials.

#### A. Stanene Preparations

High quality tin oxide was synthesized from natural  $\text{SnCl}_2 \cdot 2\text{H}_2\text{O}$  powders. In ethylene glycol after ultrasonification for 1 h, it is followed by the addition of 0.1 mmol  $\text{SnCl}_2 \cdot 2\text{H}_2\text{O}$  powders. The mixture is vigorously stirred for a fixed time period, and then transferred to a Teflon lined autoclave of the required size, which is sealed and maintained in an oven at  $160^\circ\text{C}$  for 6 h. Afterwards, the black precipitates compound are collected, washed with DI water and ethanol to eradicate the impurities. These impurities are isolated by vacuum filtration. The product is then dried in a vacuum oven at  $60^\circ\text{C}$ , and further sintered at  $300^\circ\text{C}$  for 4 h in argon to increase the crystallinity. Then the  $\text{SnO}_2$  dispersion was drop-cast onto a thin polyethylene terephthalate (PET) substrate as shown in Figure 3 and allowed to dry for about 48 hour. The pre-dried Stanene oxide is simultaneously reduced and patterned in one step process, into a rectangle strip of the required length by Universal Laser Systems VLS2.30.



Figure 3 shows the PET substrate

#### B. Electrochemical Deposition of $\text{MnO}_2$

The electrochemical anodic deposition of  $\text{MnO}_2$  is to be carried out in  $(\text{CH}_3\text{COO})_2 \text{Mn} \cdot 4\text{H}_2\text{O}$  electrolyte at a fixed voltage (Ag/AgCl (KCl saturated)) using Pt-wire as a counter electrode and Stanene/PET substrate as a working electrode. The mass of the deposited films is controlled by adjusting the total charge passed through the electrode during the deposition process. The estimated mass loading of the deposited  $\text{MnO}_2$  film can be 10, 50, and  $100 \mu\text{g}\cdot\text{cm}^{-2}$ . To improve the crystallinity of Sn in  $\text{MnO}_2$ , the product was annealed at  $200^\circ\text{C}$  for 15 h in argon atmosphere.

### IV. Material Characterization techniques

The following materials characterization techniques can be implemented in the research paper to identify the phases, present the textural features, and determine the compositions of the as-prepared materials

#### A. X-ray Diffractometry

It is a non-destructive analytical characterization method to determine the crystal phase and structure. An X-ray beam is generated by diffract meter which hits the sample as a function of polarization, incident & scattered angle, and wavelength or energy. The Stanene/ $\text{MnO}_2$  sample's particular atomic arrangement within unit cell and this will lead to particular relative intensities which are recorded as diffraction peaks. Therefore, from the angular positions of the X-ray diffraction results the unit cell size and geometry may be resolved.

#### B. Raman Spectroscopy

It is a non-destructive spectroscopic technique used to study rotational, vibrational and other low-frequency modes in a molecular system. The laser light in the Raman Microscope focuses on the test sample and interacts with its vibrations or excitations at a molecular level, generating shifted laser photons, which are immediately recorded on a Raman spectrum. The resolution of the Raman spectra can be enhanced by accumulated scans with a longer exposed time.

**C. Scanning Electron Microscopy**

Using the excited electron beam and SEM images a sample by scanning it in a raster scan pattern. The atoms that make up the sample produce signals during each scan to deliver information about the sample's composition, surface topography and electrical conductivity.

**D. Tunneling Electron Microscopy**

In a TEM the high end electron beam is transmitted through an ultra-thin sample on a copper grid, interacting with the sample as the electrons pass through to generate images. TEMs are capable of imaging at a very high resolution to reveal information at nanometer scale, such as lattice planes, *d*-spacing, etc., so they have better resolution than SEM.

**E. Atomic Force Microscopy**

To overcome the drawback associated with Scanning & Tunneling Microscopy, a very powerful high-resolution scanning probe microscopy AFM was developed to which only deals with conducting and semiconducting samples. AFM uses electric potentials to detect surface features by conducting cantilevers, which are equipped with high-resolution silicon tips to engage with the sample surface, moving along it in different modes and returning signals as electric-potentials.

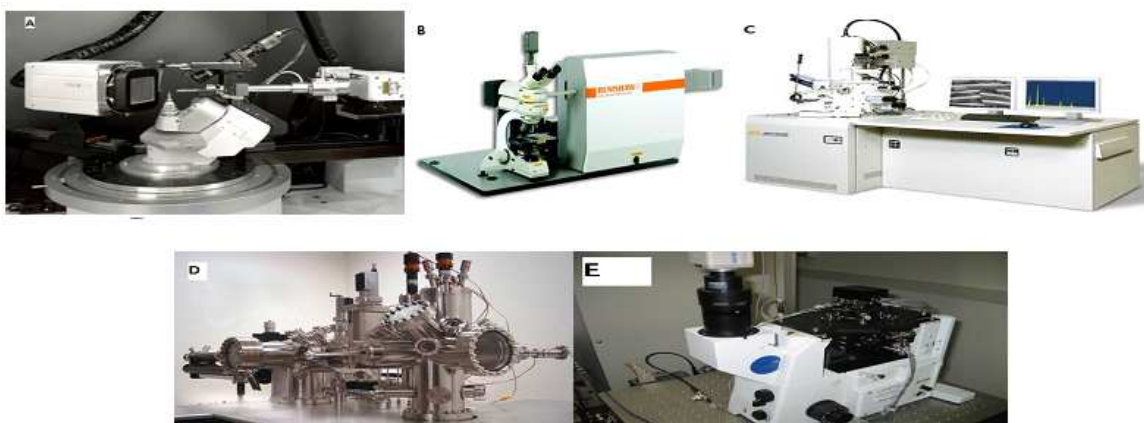


Figure 4 Steps involved in materials characterization techniques

**V. Electrochemical Characterization Techniques**

The electrical conductivity of the films of Stanene and Birnessite [5] can be calculated using the following equation 2,

$$S = \frac{10^7}{R_s * 4.532 * t_{film}} \quad (2)$$

Where *S* is the electrical conductivity (in  $S\text{ cm}^{-1}$ ),  $R_s$  is the film resistance ( $\Omega$ ) measured by a standard four-point probe system with a Kiethley 2700 Multi-meter and  $t_{film}$  is the film thickness (in nm).

**Calculations**

The capacitance values will be calculated from the CV data according to the following equation 3

$$C_{device} = \frac{1}{v(V_f - V_i)} \int_{V_i}^{V_f} I(V) dV \quad (3)$$

where  $C_{device}$  is denoted as the capacitance of the new electrode material, *v* is the scan rate (in  $V\text{ s}^{-1}$ ),  $V_f$  and  $V_i$  are the integration potential limits of the voltammetric curve and *I(V)* is the voltammetric discharge current (in amperes).

Specific capacitances would be calculated based on the area or the volume of the device stack according to the equation 4.

$$C_{area} = C_{device} / A, C_{stack} = C_{device} / V \quad (4)$$

where  $C_{area}$  (in  $F\text{ cm}^{-2}$ ) and  $C_{stack}$  (in  $F\text{ cm}^{-3}$ ) refer to the area capacitance and volumetric stack capacitance of device, respectively.  $A$  is the total area ( $\text{cm}^2$ ) and  $v$  is the volume ( $\text{cm}^3$ ) of the device. The area capacitances would be calculated based on the entire projected surface area of the device, that includes the interspaces between the micro electrodes and their area. The volumetric stack capacitances is to be calculated by taking into account the whole volume of the device, including the volume of composite electrodes, the interspaces between the electrodes, electrolyte separators, current collectors and gel electrolyte.

The electrochemical performance of the solid-state device would be shown in the Graphical plot that would be based on the volumetric stack capacitance and measured under the same dynamic condition from the discharge curves of cyclic voltammetry. The energy density of the device would be obtained from the formula given in equation 5,

$$E = \frac{1}{2} (C_{stack} * \frac{(\Delta V)^2}{3600}) \quad (5)$$

where  $E$  is the energy density (in  $\text{WH cm}^{-3}$ ),  $C_{stack}$  is the volumetric stack capacitance obtained from equation 3 and  $\Delta V$  is the discharge voltage range (in volts).

The power density of the device shall be calculated from the formula given in equation 6

$$P = \frac{E}{\Delta t} (3600) \quad (6)$$

$P$  is the power density (in  $\text{W cm}^{-3}$ ),  $E$  is the volumetric energy density and  $\Delta t$  is the discharge time (seconds).

## RESULTS AND DISCUSSION

In a composite, stanene provides chemical functionality and compatibility to allow easy processing of  $\text{MnO}_2$  in the composite. The  $\text{MnO}_2$  component mainly provides high capacity depending on its quantity, size and crystallinity. The resultant composite is not merely the sum of the individual components, but rather a new material with new functionalities and properties. From the viewpoint of structure, on one hand,  $\text{MnO}_2$  anchored or dispersed on stanene not only suppress the agglomeration and re-stacking of stanene but also increase the available surface area of the stanene alone, leading to high electrochemical activity.

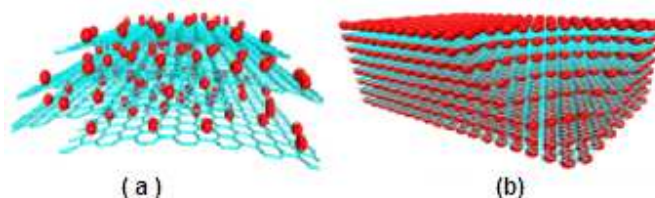


**Figure 5** Schematic of structural models of stanene/ $\text{MnO}_2$  composites: (a) Anchored model: nano-sized oxide particles are anchored on the surface of stanene. (b) Layered model: a structure composed of alternating layers of  $\text{MnO}_2$  nanoparticles and stanene. Stanene and  $\text{MnO}_2$  particles are mechanically mixed and stanene forms a conductive network among the  $\text{MnO}_2$  particles. Red:  $\text{MnO}_2$  particles; blue: stanene sheets

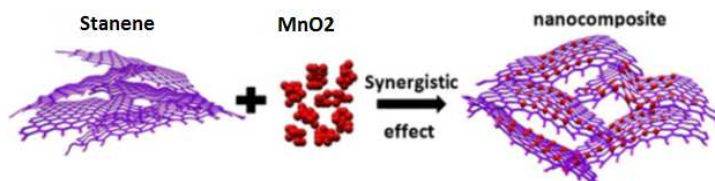


**Figure 6** Schematic of the preparation of stanene/metal oxide composites with synergistic effects between stanene and metal oxides

On the other hand, stanene as a support of  $\text{MnO}_2$  can induce the nucleation, growth and formation of fine  $\text{MnO}_2$  nano-/ microstructures with uniform dispersion and controlled morphology on the surface of stanene with high chemical functionality. The final  $\text{MnO}_2$  anchored stanene and the stanene-supported  $\text{MnO}_2$  can form a perfect integrated structure with a developed electron conductive network and shortened ion transport paths. Significant synergistic effects often occur in stanene/ $\text{MnO}_2$  composites because of size effects and interfacial interactions (a) nano-sized  $\text{MnO}_2$  anchoring on stanene; (b) stanene/ $\text{MnO}_2$  layered composites composed of aligned layers of  $\text{MnO}_2$ .

The functions and synergistic effects of stanene and  $\text{MnO}_2$  in stanene/ $\text{MnO}_2$  composites can be briefly summarized (1) stanene as a 2D support for uniformly anchoring or dispersing  $\text{MnO}_2$  with well-defined sizes, shapes and crystallinity; (2)  $\text{MnO}_2$  suppressing the re-stacking of stanene; (3) stanene acting as a 2D conductive template or building a 3D conductive porous network for improving the poor electrical properties and charge transfer pathways of pure oxides; (4) stanene suppressing the volume change and agglomeration of  $\text{MnO}_2$ ; (5) oxygen-containing groups on stanene ensures good bonding, interfacial interactions and electrical contacts between stanene and  $\text{MnO}_2$ . The hypothesis made is entirely proposed on the base of complimenting features of  $\text{MnO}_2$  and mesmerizing features of stanene which is a better conductor as compared to all group IV elements including graphene because of its stable  $\text{sp}^3$  configuration, 100% electrical conductivity and non-triviality which makes it a topological insulator. Thus we expect the proposed model to provide a 10 times better power and energy density as compared to the existing super capacitor and 3 times better as compared to existing micro super capacitor model similar to the success of Sn-  $\text{MnO}_2$  rechargeable batteries. The composed material is expected to have a good cycling stability with 90-98% of specific capacity as compared to 72% of existing MSC electrode. The details regarding the structure, topographic features, physical and chemical properties of the composite material will be published after its fabrication and its material characterization and electrochemical characterization.

## REFERENCES

- [1] Wang, Bei. "Graphene-based Nanocomposite Materials for High-performance Supercapacitors and Lithium Rechargeable Batteries." PhD diss., University of Technology Sydney, **2012**.
- [2] Li, Bing, Genhua Pan, Shakil A. Awan, and Neil Avent. *Graphene and 2D Materials* 1, no. 1 (**2014**).
- [3] Yao, Bin, Longyan Yuan, Xu Xiao, Jing Zhang, Yanyuan Qi, Jing Zhou, Jun Zhou, Bin Hu, and Wen Chen. *Nano Energy* 2, no. 6 (**2013**): 1071-1078.
- [4] Minakshi, Manickam. *Electrochemical and Solid-State Letters* 13, no. 9 (**2010**): A125-A127.
- [5] Cabana, Jordi, Laure Monconduit, Dominique Larcher, and M. Rosa Palacin. *Advanced Materials* 22, no. 35 (**2010**): E170-E192.
- [6] Dong, Xiao-Chen, Hang Xu, Xue-Wan Wang, Yin-Xi Huang, Mary B. Chan-Park, Hua Zhang, Lian-Hui Wang, Wei Huang, and Peng Chen. *ACS nano* 6, no. 4 (**2012**): 3206-3213.
- [7] Deepak, A., M. Jahnvi, K. Divya Durga, Vaidehi Ganesan, and P. Shankar. "Movement Of Robotic Arm Using Graphene Mixed Polymer Based Nanocomposite Film."
- [8] Devaraj, S., and N. Munichandraiah. *Journal of the Electrochemical Society* 154, no. 2 (**2007**): A80-A88.